ARCHITECTURAL RESEARCH, Vol. 20, No. 1(March 2018). pp. 27-34 pISSN 1229-6163 eISSN 2383-5575

A Hydration based Model for Chloride Penetration into Slag blended High Performance Concrete

Ki-Su Shin, Ki-Bong Park and Xiao-Yong Wang
Department of Architecture Engineering, Kangwon National University, Korea

https://doi.org/10.5659/AIKAR.2018.20.1.27

Abstract To improve the chloride ingress resistance of concrete, slag is widely used as a mineral admixture in concrete industry. And currently, most of experimental investigations about non steady state diffusion tests of chloride penetration are started after four weeks standard curing of concrete. For slag blended concrete, during submerged chloride penetration tests periods, binder reaction proceeds continuously, and chloride diffusivity decreases. However, so far the dependence of chloride ingress on curing ages are not detailed considered. To address this disadvantage, this paper shows a numerical procedure to analyze simultaneously binder hydration reactions and chloride ion penetration process. First, using a slag blended cement hydration model, degree of reactions of binders, combined water, and capillary porosity of hardening blended concrete are determined. Second, the dependences of chloride diffusivity on capillary porosity of slag blended concrete are clarified. Third, by considering time dependent chloride diffusivity and surface chloride content, chloride penetration profiles in hardening concrete are calculated. The proposed prediction model is verified through chloride immersion penetration test results of concrete with different water to binder ratios and slag contents.

Keywords: Chloride Penetration, Slag Blended Cement, Hydration, Hardening Concrete, Model

1.INTRODUCTION

Corrosion of steel rebar is a common degrading mechanism for reinforced concrete (RC) structures at close to marine environment. Corrosion of reinforcement causes defects of RC structures. The concrete cover of reinforcement will spall off, and the cross section, yield strength, and ductility of the reinforcement will be reduced, and the bonding strength between steel rebar and concrete will be impaired. Hence load bearing capacity and serviceability may be reduced (Shi et al. 2012).

Blast furnace slag (BFS) is a by-product of steel industry. The chemical compositions of granulated slag is similar with that of cement, and slag has been widely used a mineral admixtures to produce high performance concrete. Slag blended concrete shows advantages in restraining chloride ion ingression and improving concrete resistance about chloride ion penetration. The experimental investigations and theoretical modeling about chloride ingress resistance of slag blended concrete are abundant. Using water to binder ratio of concrete, Life-365 program (2018) evaluated chloride diffusion coefficients at 28 days curing age. Papadakis (2000) calculated the total porosity of concrete containing supplementary cementitious materials and evaluated the chloride diffusivity as a function of porosity and paste contents. By using chloride diffusion coefficient proposed by Papadakis (2000), Vu and Stewart (2000) predicted chloride ingression of concrete structures in coastal zone and application of de-icing salts environment. However, it should be noticed that Life-365 program (2018) and Papadakis (2000) assume that all the binder will hydrate regardless of water to binder ratios. Wang (2014) reported that with the reduction of water to cement ratios, rate of hydration and final degree of hydration decrease.

Using the reaction degree of cement, Nielsen and Geiker (2003) calculated phase volume fractions of hydrating concrete, such as chemically shrinkage, capillary water, and solid products. Furthermore, chloride diffusivity in paste and concrete were determined using phase volume fractions and aggregate contents. Sun et al. (2011) proposed a multi scale model for predicting chloride diffusion coefficient of concrete. Microstructure of harden cement paste and interfacial transition

Corresponding Author: Xiao-Yong Wang
Department of Architecture Engineering,
Kangwon National University, Chuncheon, South Korea
e-mail: wxbrave@kangwon.ac.kr

This research was supported by Basic Science Research Program through the National Research Foundation of Korea(NRF) funded by the Ministry of Science, ICT & Future Planning(No.2016R1A2B4013596) and partially supported by 2017 Research Grant from Kangwon National University (No. 520170127).

zone (ITZ) is introduced into model proposed. However, Nielsen and Geiker's model (2003) and Sun et al's model (2011) are only valid for Portland cement concrete. The influences of mineral admixtures on chloride diffusion coefficient are not taken into account. By using reaction degrees of cement and silica fume, Song et al. (2007) calculated capillary porosity and chloride diffusivity in bulk paste and ITZ. Furthermore, diffusivity of concrete are determined by considering effects of bulk paste, ITZ, and aggregate. By using general effective media equation, Oh and Jang (2004) calculated chloride diffusivity in bulk paste. Furthermore, chloride diffusivity of concrete is calculated using composite spheres assemblage model considering influences of paste matrix, aggregate, and ITZ. However, Song et al. (2007) and Oh and Jang (2004)'s model do not consider the evolution of capillary porosity and are only valid for fully hardened concrete. For Song et al. (2007) and Oh and Jang (2004)'s model, more improvements are necessary for considering the effects of ages.

And currently, most of experimental investigations about non steady state diffusion tests of chloride penetration are started after four weeks standard curing of concrete. For slag blended concrete, during submerged chloride penetration tests periods, binder reaction proceeds continuously, and chloride diffusivity decreases. However, so far the dependence of chloride ingress on curing ages are not detailed considered. An empirical parameter (Song and Kwon 2009) is widely used to describe the evolution of chloride diffusion coefficient with curing ages. While this empirical time parameter cannot fully describe the evolution of hardening concrete microstructure. The influence of various factors such as cement type, water-to-binder ratio, and fly ash replacement ratio on this empirical time parameter requires further investigation.

To address the disadvantages of current models, this paper presents a prediction model to analyze simultaneously binder reaction and chloride penetration process. By combining blended cement hydration model with chloride penetration model, the dependences of evaporable water, capillary porosity, and chloride diffusivity on age of slag blended concrete are clarified. Furthermore, by considering time dependent chloride diffusivity and surface chloride content, chloride penetration profiles in slag blended hardening concrete are determined.

2. CEMENT HYDRATION MODEL AND CHLORIDE INGRESS MODEL

2.1 Slag Blended Cement hydration model

Wang (2014) proposed a hydration model for concrete containing supplementary cementitious materials, such as fly ash, slag, and silica fume. Hydration equations for cement and mineral admixtures are respectively proposed, and the mutual interactions between cement hydration and mineral admixtures reaction are considered through capillary water contents and calcium hydroxide contents. The hydration model is valid for concrete with different water to binder ratios, mineral admixture replacement ratios, and curing temperatures

Reaction degrees of cement and mineral admixture are used as fundamental indicators to evaluate properties development of concrete. Degree of cement hydration (α) is defined as the ratio of mass of hydrated cement to mass of cement in the mixing proportion. The value of degree of cement hydration (α) ranges between 0 and 1. Degree of cement hydration α=0 means hydration does not start, and degree of cement hydration α=1 means cement has fully hydrated.

By using an integration method, degree of cement hydration can be determined as follows:

$$\alpha = \int_0^t \left(\frac{d\alpha}{dt} \right) dt \tag{1}$$

where t is time, $\frac{d\alpha}{dt}$ is rate of cement hydration. The detailed equations for $\frac{d\alpha}{dt}$ are available in our former research (Wang 2014)).

Similarly, reaction degree of mineral admixture (α_M) is defined as the ratio of mass of reacted mineral admixture to mass of mineral admixture in the mixing proportion. The value of reaction degree of mineral admixture (α_M) ranges between 0 and 1. α_M=0 means mineral admixture reaction does not start and α_M=1 means all the mineral admixture has reacted. Reaction degree of mineral admixture also can be determined using an integration method in time domain as follows:

$$\alpha_M = \int_0^t \left(\frac{d\alpha_M}{dt} \right) dt \tag{2}$$

where $\frac{d\alpha_M}{dt}$ is rate of mineral admixture reaction. The detailed equations for $\frac{d\alpha_M}{dt}$ are available in our former research (Wang 2014)).

Based on mixing proportions and reaction degree of binders, the phase volume fractions of hardening slag blended concrete can be determined as follows (Wang 2014):

$$V_1 = \frac{C_0}{\rho_c}(1-\alpha) \tag{3}$$

$$V_2 = \frac{P}{\rho_{SG}}(1-\alpha_M) \tag{4}$$

$$V_3 = 0.4*C_0*\alpha + 0.45*\alpha_M*P \tag{5}$$

$$V_4 = W_0 - V_3 \tag{6}$$

$$V_5 = V_4 + 0.0625*C_0*\alpha + 0.10*\alpha_M*P \tag{7}$$

$$V_6 = V_4 + 0.15*C_0*\alpha + 0.15*\alpha_M*P \tag{8}$$

$$V_7 = 1 - V_1 - V_2 - V_3 - V_a \tag{9}$$

where V_1, V_2, V_3, V_4, V_5, V_6, and V_7 are volume fractions of unhydrous cement, unreacted slag, combined water, capillary water, capillary porosity which equals to the sum of capillary water and chemically shrinkage, evaporable water which equals to the sum of gel water and capillary water, and reaction products, respectively. C_0 is mass of cement in the mixing proportions, ρ_c is density of cement, P is mass of slag in mixing proportion, ρ_{SG} is density of slag, W_0 is mass of water in the mixing proportions, and V_a is volume of aggregate. In equation (5), $0.4*C_0*\alpha$ and $0.45*\alpha_{Af}*P$ are combined water from cement hydration and from slag reaction respectively. In equation (7), $0.0625*C_0*\alpha$ and $0.10*\alpha_{Af}*P$ are chemical shrinkage from cement hydration and from slag reaction respectively. In equation (8), $0.15*C_0*\alpha$ and $0.15*\alpha_{Af}*P$ are gel water from cement hydration and from slag reaction respectively.

2.2 Chloride diffusion coefficient model

Concrete is a three phase material consisting of cement paste matrix, aggregate, and interfacial transition zone (ITZ) between cement paste matrix and aggregate. Interfacial zones are formed due to the wall effect and one sided growth of the cement particles. Cement paste matrix is connected with interfacial transition zone. The diffusivity of cement paste phase D_p is mainly dependent on capillary pores of the cement paste, and can be determined as follows (Oh and Jang 2004):

$$D_P(t) = A_1 * (\phi_{paste})^{A_2} \tag{10}$$

$$\phi_{paste} = \frac{V_5}{\frac{C_0}{\rho_c} + \frac{P}{\rho_{SG}} + W_0} \tag{11}$$

where A_1 and A_2 are the relation coefficients between the capillary porosity and chloride diffusivity, ϕ_{paste} is the capillary porosity in the binder paste. In equation (10), intrinsic diffusion coefficient A_1 relates to type of binders, such as cement or slag. Exponent A_2 ($A_2 > 1$) relates to pore size distribution or complexity of microstructure of reaction products.

When the diffusivity of the aggregate particle inclusions is assumed to be zero, according to composite sphere assemblage (CSA) model (Oh and Jang 2004), the chloride diffusion coefficient of concrete can be determined as follows:

$$\frac{D_c}{D_P} = 1 + \frac{V_a}{\frac{1}{2(D_i / D_P)\varepsilon - 1} + \frac{1 - V_a}{3}} \tag{12}$$

where D_c is the diffusivity of concrete, D_i is the diffusivity in the interfacial transition zone, and ε is thickness ratio of ITZ. As shown in equations (10)-(12), with the proceeding of binder hydration, the capillary porosity of concrete decreases, and the chloride diffusion coefficient decreases correspondingly.

By using hard core/soft shell model, Bentz et al. (1999) evaluated the connectivity of interfacial zones for different choices of interfacial zone thickness. Furthermore, by comparing against with cement mortar mercury intrusion data, it was found that a choice of 20μm for the interfacial zone thickness gave the best agreement with the mercury data (Bentz et al 1999). The mean radius of coarse aggregate is about 10 mm. Hence in this study, the thickness ratio of ITZ is used about ε =0.002.

Bentz et al. (1999) studied the effects of mineral admixtures on interfacial transition zone. They found that for fly ash blended mortar, the fraction ratio of CSH between ITZ and bulk matrix is similar with that in plain cement mortar. Similarly, based on analysis about chloride diffusivity of concrete with various fly ash and slag additions, Oh and Jang (2004) proposed that for Portland cement concrete, fly ash blended concrete, and slag blended concrete, the ratios between D_i and D_p are almost same ($D_i / D_p = 7$).

The effects of slag additions on chloride diffusion coefficients of concrete are summarized as follows: first, incorporating GGBS into blended binders can increase total porosity because the reactivity of slag is lower than that of cement. This point is considered using slag blended cement hydration models (equations (1)-(9)); second, calcium silicate hydrate (CSH) gel produced from slag reaction has finer gel pores than that from cement hydration. This effect is considered using intrinsic diffusion coefficient A_1 in equation (10); third, the formation of slag reaction products can fill large capillary voids and reduce the average pore size. This effect is considered using chloride diffusion exponent A_2 in equation (10). It should be noticed that in our study, the evolution of chloride diffusion coefficient is directly related to time-dependent capillary porosity. We do not use the empirical time parameter (Song and Kwon 2009) to describe the age dependence of the chloride diffusion coefficient. Compared with empirical time parameter method (Song and Kwon 2009), the physical meaning of proposed model in this study is much clearer.

2.3 Time dependent surface chloride content

Nagataki et al. (1993) measured water soluble chloride concentration of pore solution in the surface of concrete specimen. They found that chloride concentration of pore solution increases with the immersion period. At an immersion period of 90 days, the chloride concentration of pore solution is almost twice as high as that of the immersion solution. After 90 days, the chloride concentrations of solutions are still in an increasing trend. Baroghel-Bouny et al.(2007) also found that

for concrete specimens, after 90 days non-steady-state diffusion tests, the ratio between chloride concentration of surface concrete pore solution and chloride concentration of contact external solution is about 2.2, which generally agree with Nagataki et al's results (1993).

The chloride condensation index is defined as the chloride concentration of the pore solution in the specimens divided by the chloride concentration of the surrounding solution in which the specimen is immersed. Based on Nagataki et al's results (1993), we propose that chloride condensation index can be determined as follows:

$$CI = 0.8 + 0.022t / (1 + 0.013t) \quad (13)$$

where CI is chloride condensation index, and t is immersion period (days). As shown in Figure 1, condensation index increases quickly at initial immersion periods. At late ages, the increase of condensation index is marginal.

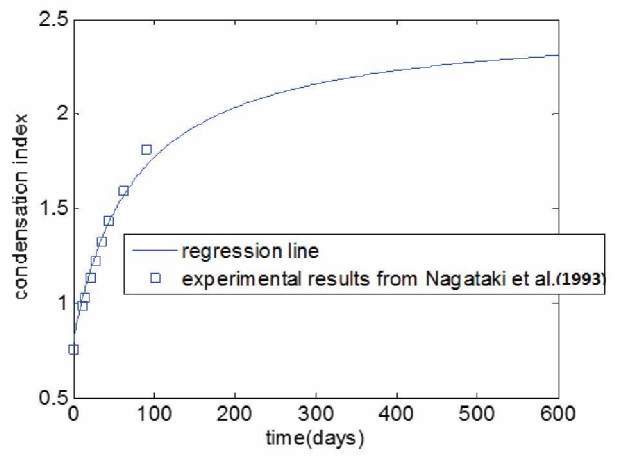

Figure 1. chloride concentration condensation index

2.4 Governing equation of Chloride diffusion

For saturated concrete, chloride ions can penetrate concrete through ionic diffusion. The ionic diffusion comes from the existing concentration gradient between exposed environment and pore soltuion of concrete. This process can be described using Fick's 1st law as follows (Maekawa et al 2009):

$$J_c = -D_e V_6 \frac{\partial C_f}{\partial x} \quad (14)$$

where J_c denotes the flux of chloride ions in concrete due to diffusion (kg/m^2·s); C_f denotes free chloride concentration at depth x(m) (the unit of C_f is kg/m^3 of pore solution).

In saturated concrete, the mass conservation of chloride ions can be determined using Fick's second law, as follows (Maekawa et al 2009):

$$\frac{\partial C_t}{\partial t} = -\nabla \cdot J_c \quad (15)$$

where C_t denotes the total chloride concentration (the unit of C_t is kg/m^3 of concrete).

Chlorides present in concrete consists of free chloride and bound chloride. Free chlorides refer to dissolved chloride ions in the pore liquid. Free chlorides exist in a freely mobile state. Bound chlorides include solid phase chloride and adsorbed chloride. Bound chlorides can not move at ordinary chloride concentration gradient. The relations among total chloride concentration, bound chloride concentration, and free chloride concentrations are shown as follows (Maekawa et al 2009):

$$C_t = C_b + V_6 * C_f \quad (16)$$

Where C_b denotes the concentration of bound chlorides (the unit of C_b is kg/m^3 of concrete). The evaporable water contents V_6, can be determined from hydration model using equation (8).

By substituting equations (15)-(16) into equation (14), Ficks second law can be modified as follows:

$$\frac{\partial C_f}{\partial t} = \frac{\partial}{\partial x}\left(\frac{D_e}{1 + \frac{1}{V_6}\frac{\partial C_b}{\partial C_f}} \frac{\partial C_f}{\partial x} \right) \quad (17)$$

where $\partial C_b / \partial C_f$ denotes the binding capacity of the concrete binder. As shown in equation (17), chloride penetration process relates to some factors, such as chloride diffusion coefficient, chloride binding isotherm, and evaporable water contents in concrete.

2.5 Nonlinear chloride binding model

Diffusing chloride ions are physically bound and chemically bound onto pore surfaces within cement matrix (Maekawa et al 2009). The relationships between bound chlorides and free chlorides can be described using binding isotherms. Chloride binding isotherms relates to chemical compositions cementitious system and surrounding environmental conditions. By measuring free chloride and bound chloride contents for slag blended concrete, Maekawa et al.(2009) proposed that under equilibrium condition, the relationship between free chloride ions and bound chlorides is modeled as Langmuir type equation as follows:

$$C_b = \frac{\chi C_f}{1 + 4C_f} \quad (18)$$

$$\chi = -34b^2 + 23.3b + 11.8 (0 \le b \le 0.6) \quad (19)$$

where b is slag replacement ratio. In equation (18), the unit of free chloride and bound chloride is weight percentage by mass of binder. In equation (18), b=0 means Portland cement concrete.

2.6 Boundary condition and initial condition of chloride ingress

The initial condition and boundary condition used in proposed model are shown as follows:

$$\text{For } t=0: \quad C_f = C_0 \text{ at } x>0 \tag{20}$$

$$\text{For } t\geq 0: \quad C_f = CI * C_s \text{ at } x=0 \tag{21}$$

$$\frac{\partial C_f}{\partial x} = 0 \text{ at } x=L/2 \text{ (axis of symmetry)} \tag{22}$$

where C_0 is chloride concentration in the pore solution before the concrete is exposed to an external salt solution, C_s is the chloride ion concentration of salt solution in contact with the concrete outer surface (equation (21) considers chloride concentration condensation), and L is the thickness of the member.

2.7 Summary of proposed model

The proposed numerical procedure considers the interactions between cement hydration and chloride penetrations. The steps of proposed numerical procedures are shown as follows:

First, using a blended cement hydration model, degree of binder reactions and phases volume fractions of hardening concrete, such as evaporable water content, combined water, and capillary porosity are determined.

Second, the dependences of chloride diffusivity and surface chloride content on age of concrete are clarified. Chloride diffusion coefficient of hardening concrete is calculated considering the evolution of capillary porosity in binder paste and composite sphere assemblage (CSA) model. By using chloride condensation index, the evolution of surface chloride content is clarified. Chloride binding of slag blended concrete is described using Langmuir binding isotherm.

Third, chloride profiles in hardening concrete are calculated. Governing equation of chloride diffusion (equation (17)) and in time is an initial-value problem and in space is a boundary-value problem. In this study, finite element method is used to solve this equation.

3. VERIFICATION OF PROPOSED MODEL

Experimental results from Song and Kwon (2009) are used to verify the proposed model. Song and Kwon (2009) made systematically experimental study about chloride ingress of slag blended concrete. They measured chloride diffusion coefficients and chloride penetration profile of slag blended concrete with various mixing proportions. Concrete specimens with three different water-to-binder ratios of 0.47, 0.42, and 0.37 and two different slag contents of 30% and 50% were prepared. Concrete cylinder specimens were cured in moist conditions.

Measurement of chloride diffusion coefficient: At the curing periods of 28 days (four weeks), 90 days (three months), 180 days (six months), and 270 days (nine months), chloride diffusion coefficients are measured through an electrical accelerated method. After the electrical accelerated test, a silver nitrate solution ($AgNO_3$ with a concentration of 0.1 mol/l) is used as an indicator to measure chloride penetration depth, and the chloride diffusion coefficient is calculated through the penetration depth (Song and Kwon 2009).

Measurement of total chloride contents: After 28 days of curing, the specimens are immersed in a 3.5% NaCl solution for 6 months. The specimens are coated with resin, except for the upside surface that allows for a one-dimensional intrusion of chloride ions. Acid-soluble chloride contents (which equal to total chloride contents) are measured at different penetration depths (Song and Kwon 2009).

3.1 Capillary porosity

In hydrating cement-slag blends, with the increasing of combined water, reaction products deposit in capillary pore space, and capillary porosity decreases. Figure 2 shows the amount of capillary porosity in binder paste as functions of curing ages. As shown in Figure 2, when water to binder ratio increases from 0.37 to 0.47, the amount of capillary porosity increases. For concrete containing 50% slag, the amount of capillary porosity is higher than that in plain concrete.

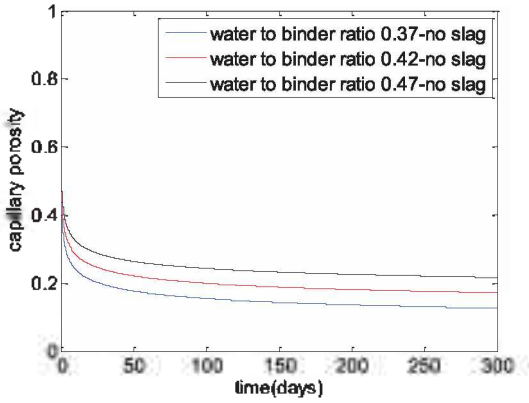

(2-a) plain concrete

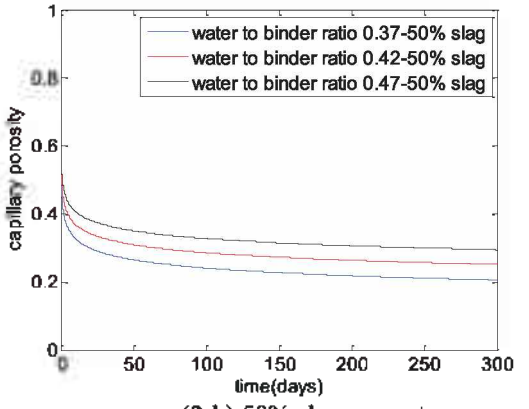

(2-b) 50% slag concrete

Figure 2. capillary porosity

3.2 Evaluation of chloride diffusion coefficients and chloride ingress profile for slag blended concrete

As mentioned in section 2.2, the intrinsic diffusion coefficient A1 and exponent A2 in equation (10) is dependent on water to binder ratios, and only relates to type of binders. We assumed that cement and slag contribute to intrinsic diffusion coefficient A1 and exponent A2 relating to binder weight fractions as follows:

$$A_1 = B_1 * \frac{C_0}{C_0 + M_0} + B_2 * \frac{M_0}{C_0 + M_0} \quad (23)$$

$$A_2 = C_1 * \frac{C_0}{C_0 + M_0} + C_2 * \frac{M_0}{C_0 + M_0} \quad (24)$$

where B_1 and B_2 are the contributions of cement and slag on intrinsic diffusion coefficient A_1 respectively; and C_1 and C_2 are the contributions of cement and slag on exponent A_2, respectively. $\frac{C_0}{C_0+M_0}$ and $\frac{M_0}{C_0+M_0}$ are the weight fractions of cement and slag in cement-slag blends respectively. As shown in Eq. (23) and (24), when the replacement ratio of slag equals to zero, the chloride diffusion coefficient is only dependent on the values of B_1 and C_1, which relate to cement; when slag is used as a mineral admixture, the chloride diffusion coefficient is dependent on the values of B_1, B_2, C_1, and C_2.

Using experimental results about chloride diffusion coefficients measured at different ages for various mixing proportions, the values of B_1, B_2, C_1, and C_2 are calibrated as 3.90e-10 ,0.72e-10, 1.21 and 2.31 respectively. As shown in Figure 3, the analyzed results general agree with experimental results. The correlation coefficient between analyzed results and experimental results is 0.96. The addition of slag can reduce the intrinsic chloride diffusion coefficient A_1 (because of $B_1 > B_2$). This is because the gel produced from slag reaction has finer gel pores than from cement hydration. In addition, the addition of slag can increase the chloride diffusion exponent A_2 (because of $C_1 < C_2$). This may be due to the pore-size refinement effect resulting from the slag reactions. With the reduction of intrinsic chloride diffusion coefficient A_1 and increase of the chloride diffusion exponent A_2, chloride diffusion coefficients decrease correspondingly.

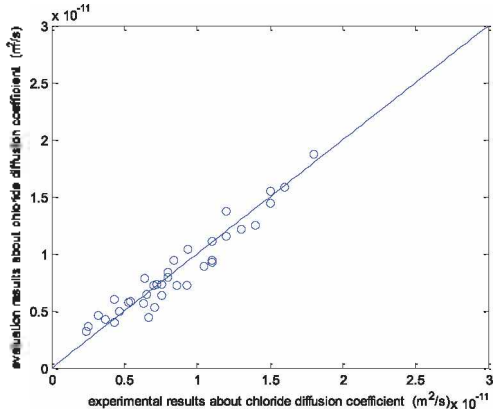

Figure 3. comparisons between experimental results and analyzed results of chloride diffusion coefficient

The calculated total chloride concentration profiles are shown in Figure 4. The calculated results generally agree with experimental results. As shown in Figure 4-a, with the increasing of water to cement ratios, due to the reductions of chloride diffusion coefficients, given the same depth the chloride ions concentration will decrease. As shown in Figure 4-b and 4-c, compared with that of Portland cement concrete, because of the reduction of chloride diffusion coefficients and increasing of chloride binding capacity, the additions of slag can reduce chloride penetration depth.

Figure 5 shows the effect of chloride concentration condensation on chloride penetration profile. In this calculation, the concentration condensation is ignored (CI =1), and the boundary condition at x=0 is used as $C_f = C_s$ in equation (21). As shown in Figure 5, the chloride contents in the surface zone are much lower than experimental results, and chloride ingress depths are similar with that shown in Figure 4. Hence chloride concentration condensation mainly affect chloride contents in the surface zone of concrete.

Figure 6 shows the effect of chloride binding on chloride penetration profile. In this calculation, the chloride binding capacity is ignored (χ =0), and the binding capacity is used as C_b =0 in equation (18). As shown in Figure 6, the chloride contents in concrete are much lower than experimental results, and chloride ingress depths are much higher than that shown in Figure 4. Hence chloride binding presents significant influences on chloride content and chloride penetration depth.

4. CONCLUSIONS

This paper presents a numerical procedure to analyze chloride penetration into hardening slag blended concrete. The simultaneous binders hydration reaction and chloride ion penetration process are modeled.

First, using a slag blended cement hydration model, degree of binders reaction and phases volume fractions of hardening concrete, such as evaporable water content, combined water, and capillary porosity, are determined.

Second, a general equation of chloride diffusion coefficient for hardening slag blended concrete are proposed. The increasing total porosity due to slag addition, the pore refinement at macro-scale by slag due to filling effect, and the pore refinement at micro-scale due to latent-hydraulic property and pozzolanic reaction of slag are analyzed.

Third, by using numerical analysis method, chloride profiles in hardening concrete are calculated. Analysis results generally agree with experimental results of concrete with different curing ages and different mixing proportions. Because of the reduction of chloride diffusion coefficients and increasing of chloride binding capacity, the additions of slag can reduce chloride penetration depth. Chloride concentration condensation mainly affect chloride contents in the surface zone of concrete. Chloride binding presents significant influences on chloride content and chloride penetration depth.

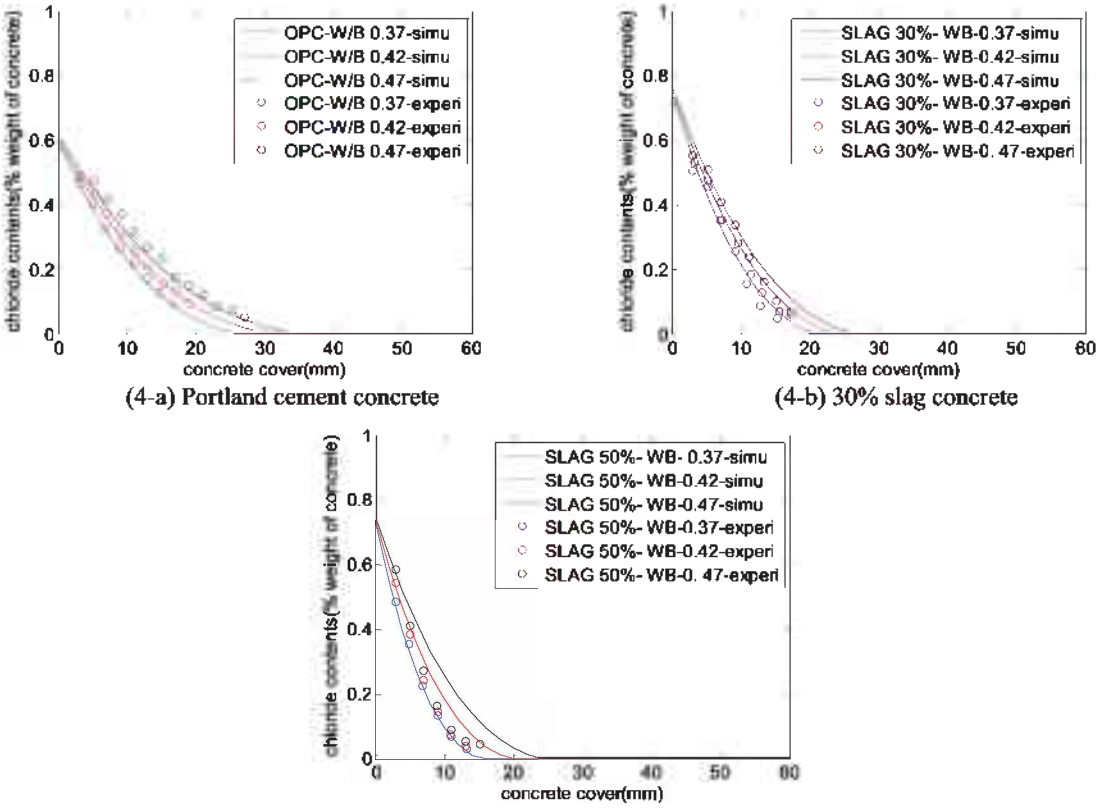

(4-a) Portland cement concrete

(4-b) 30% slag concrete

(4-c) 50% slag concrete.

Figure 4. Chloride ingress profiles in slag blended concrete

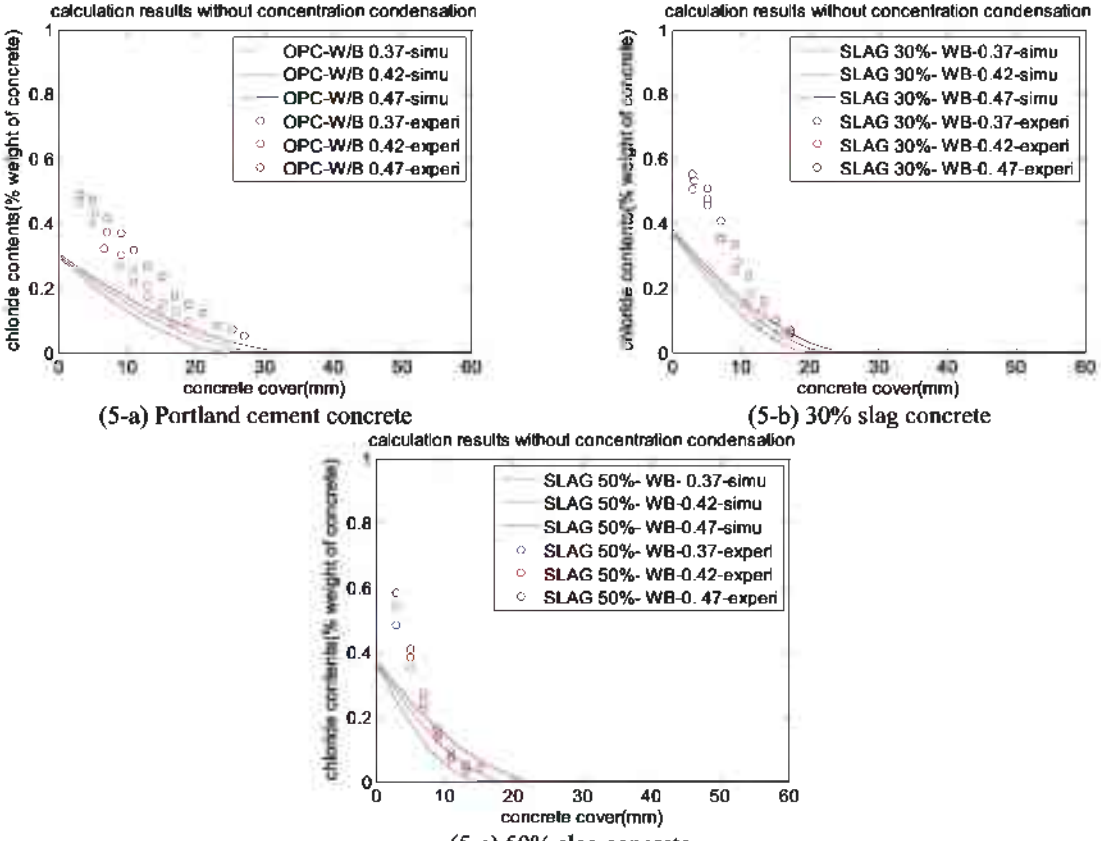

(5-a) Portland cement concrete

(5-b) 30% slag concrete

(5-c) 50% slag concrete.

Figure 5. Chloride ingress profiles in slag blended concrete without concentration condensation effect

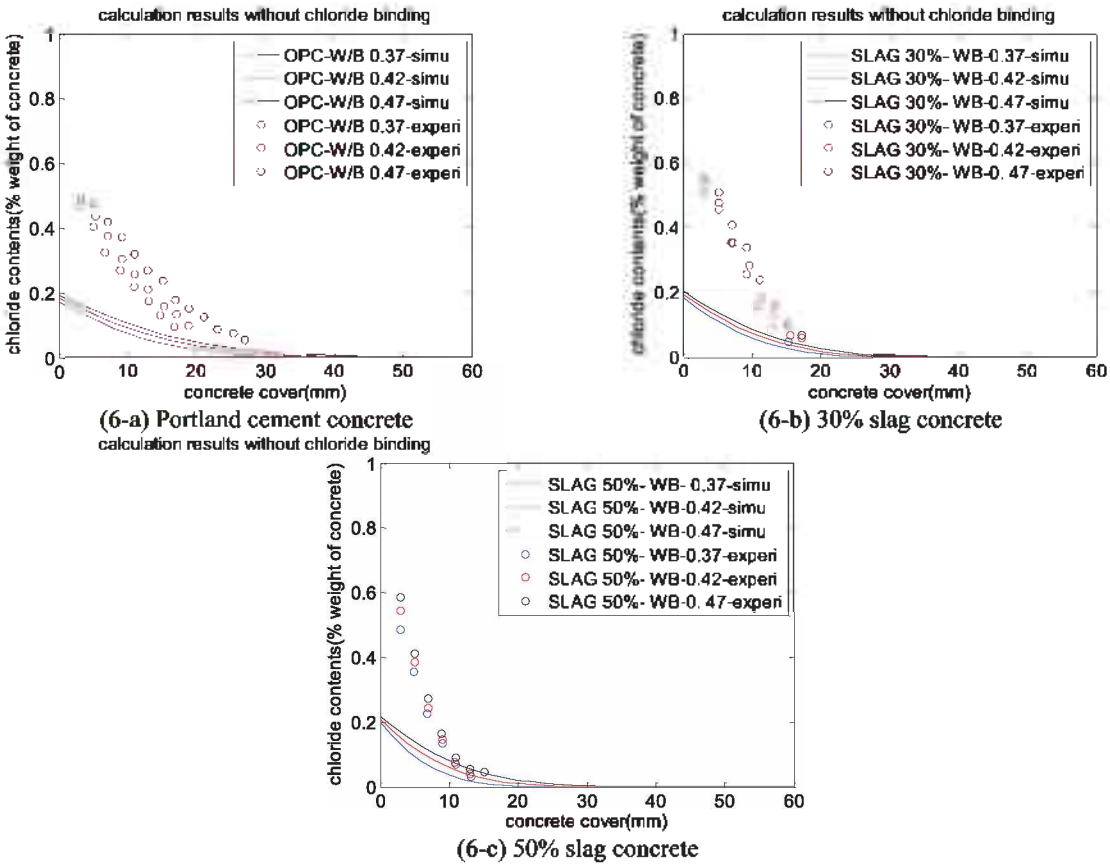

Figure 6. Chloride ingress profiles in slag blended concrete without chloride binding effect

REFERENCES

Baroghel-Bouny V, Belin P, Maultzsch M, Henry D (2007). AgNO3 spray tests: advantages, weaknesses, and various applications to quantify chloride ingress into concrete. Part 1: Non-steady-state diffusion tests and exposure to natural conditions. Materials and Structures, 40,759–781

Bentz DP, Garboczi EJ(1999). A hard core/soft shell microstructural model for studying percolation and transport in three dimensional composite media. NISTIR 6265, National institute of standards and technology

Maekawa K, Ishida T, Kishi T(2009), Multi-scale Modeling of Structural Concrete, Taylor & Francis, London.

Nagataki S, Otsuki N, Wee TH, Nakashita K (1993). Condensation of Chloride Ion in Hardened Cement Matrix Materials and on Embedded Steel Bars. ACI Materials Journal, 90,323-332

Nielsen EP, Geiker MR (2003). Chloride diffusion in partially saturated cementitious material. Cement and Concrete Research, 33 ,133 – 138

Oh BH, Jang SY (2004). Prediction of diffusivity of concrete based on simple analytic equations. Cement and Concrete Research, 34,463–480

Papadakis VG (2000). Effect of supplementary cementing materials on concrete resistance against carbonation and chloride ingress. Cement and Concrete Research, 30,291–299

Shi XM, Xie N, Fortune K, Gong J (2012). Durability of steel reinforced concrete in chloride environments: An overview. Construction and Building Materials, 30,125–138

Song HW, Kwon SJ (2009). Evaluation of chloride penetration in high performance concrete using neural network algorithm and micro pore structure. Cement and Concrete Research, 39,814-824.

Song HW, Jang JC, Velu S, Byun KJ (2007). An estimation of the diffusivity of silica fume concrete. Building and Environment 42, 1358–1367

Sun GW, Zhang YS, Sun W, Liu ZY, Wang CH(2011). Multi-scale prediction of the effective chloride diffusion coefficient of concrete. Construction and Building Materials, 25, 3820–3831

Vu K, Stewart MG (2000). Structural reliability of concrete bridges including improved chloride-induced corrosion models. Structural Safety 22, 313–333

Wang XY (2014). Effect of fly ash on properties evolution of cement based materials. Construction and Building Materials, 69, 32–40

www.life-365.org/ (2018)

(Received Dec. 12, 2017/Revised Mar. 16, 2018/Accepted Mar. 20, 2018)